Dirac Equation in (1 + 1)-Dimensional Curved Spacetime and the Multiphoton Quantum Rabi Model

J. S. Pedernales,[1,2] M. Beau,[3] S. M. Pittman,[4] I. L. Egusquiza,[5] L. Lamata,[1] E. Solano,[1,6,7] and A. del Campo[3]
[1]Department of Physical Chemistry, University of the Basque Country UPV/EHU, Apartado 644, 48080 Bilbao, Spain
[2]Institute for Theoretical Physics and IQST, Albert-Einstein-Allee 11, Universität Ulm, D-89069 Ulm, Germany
[3]Department of Physics, University of Massachusetts, Boston, Massachusetts 02125, USA
[4]Department of Physics, Harvard University, Cambridge, Massachusetts 02138, USA
[5]Department of Theoretical Physics and History of Science, University of the Basque Country UPV/EHU, Apartado 644, 48080 Bilbao, Spain
[6]IKERBASQUE, Basque Foundation for Science, Maria Diaz de Haro 3, 48013 Bilbao, Spain
[7]Department of Physics, Shanghai University, 200444 Shanghai, China

(Received 29 July 2017; revised manuscript received 25 January 2018; published 17 April 2018)

We introduce an exact mapping between the Dirac equation in $(1 + 1)$-dimensional curved spacetime (DCS) and a multiphoton quantum Rabi model (QRM). A background of a $(1 + 1)$-dimensional black hole requires a QRM with one- and two-photon terms that can be implemented in a trapped ion for the quantum simulation of Dirac particles in curved spacetime. We illustrate our proposal with a numerical analysis of the free fall of a Dirac particle into a $(1 + 1)$-dimensional black hole, and find that the *Zitterbewegung* effect, measurable via the oscillatory trajectory of the Dirac particle, persists in the presence of gravity. From the duality between the squeezing term in the multiphoton QRM and the metric coupling in the DCS, we show that gravity generates squeezing of the Dirac particle wave function.

DOI: 10.1103/PhysRevLett.120.160403

Introduction.—The simulation of gravitational theories and related phenomena in the laboratory constitutes an ongoing effort that spans decades of research. Following Unruh's seminal work [1] to study Hawking radiation using a sonic analog of a black hole, a variety of systems for the analog simulation of gravity have been put forward. Prominent examples include classical fluids [2–4], shallow water waves [5–7], Bose-Einstein condensates [8–19], ultracold atoms in optical lattices [20], superfluid helium [21–23], nonlinear electrodynamics [24–28], slow light [29–32], waveguides [33,34], ion rings [35], and laser filaments [36,37]; see Refs. [38,39] for an extensive review. In the same manner, embedding quantum simulators have recently been identified as suitable candidates for the quantum simulation of Rindler transformations, allowing for the observation of black hole physics and related relativistic phenomena in the lab [40].

In parallel, the field of quantum optics provides a plethora of controllable quantum systems as potential quantum simulators. This has led to a number of analogies between models of quantum optics and other fields of physics. A paradigmatic example is the connection between the quantum Rabi model (QRM), which describes light-matter interaction, and relativistic quantum physics. The simulation of a Dirac fermion in Minkowski spacetime has been proposed and implemented in several platforms [41–45]. However, the connection between quantum optics and quantum theory in curved spacetime remains unexplored. In this Letter, we complete this missing link by establishing an analogy between a multiphoton QRM and a Dirac particle in a $(1 + 1)$-dimensional curved spacetime (DCS), which highlights the connection between the two fields. After introducing an exact mapping from a Dirac particle in the background of a $(1 + 1)$-dimensional black hole [46] to the multiphoton QRM, we propose its implementation in a trapped-ion platform. Using numerically exact calculations, we explore the dynamics of a massive Dirac particle in the vicinity of a black hole through the analogy between the multiphoton QRM and DCS. Our results show evidence of the *Zitterbewegung* effect in the trajectory of the particle and its density profile. Finally, we demonstrate that gravitation squeezes quantum states as time evolves, in agreement with some recent results [47–50].

The quantum Rabi model and the Dirac equation.—The QRM describes the interaction of a two-level atom with a quantized mode of the electromagnetic field. When the wavelength of the electromagnetic mode greatly exceeds the size of the atom, the dipolar approximation that neglects the spatial dependence of the electromagnetic field justifies a linear atom-field interaction. Interactions that are quadratic in the field emerge in the description of effective two-level systems due to second-order processes mediated by a virtual third level that is negligibly populated. When the atom-field coupling includes both linear and quadratic terms in the field operators, the Hamiltonian reads ($\hbar = 1$)

$$H_R = \omega \hat{a}^\dagger \hat{a} + \frac{\omega_0}{2}\sigma_z + g\sigma_x(\hat{a} + \hat{a}^\dagger) + \kappa\sigma_x(\hat{a}^2 + \hat{a}^{\dagger 2}), \quad (1)$$

where ω is the mode frequency, ω_0 the energy splitting of the two level system, and g and κ are the coupling strengths of the linear and quadratic terms, respectively. The linear QRM has been proposed and implemented in all its parameter regimes using trapped ions [43,51] and in the ultrastrong and deep-strong coupling regimes using superconducting circuits [52–54], with protocols that can be as well extended to nonlinear cases [55]. For $\kappa = 0$ and $\omega = 0$, the corresponding Schrödinger equation is equivalent to the $(1+1)$-dimensional Dirac equation in flat Minkowski spacetime, $i\partial_t\psi = (mc^2\sigma_z + p\sigma_x)\psi$, upon identifying $\omega_0/2 = mc^2$ and $g = cp_0$. Here, p_0 is the dimensional part of the momentum operator $p = p_0(a - a^\dagger)/i$. This analogy has been exploited in trapped ions for the quantum simulation of relativistic fermions in flat spacetimes [42,56]. In this Letter, we argue that the analogy holds when a static gravitational field is included provided that the QRM contains a quadratic two-photon term.

First, let us recall the general form of the DCS for a fixed metric $g_{\mu\nu}$ in $(1+1)$-dimensional spacetime. Assume the signature $(+-)$, where $\mu = 0$ corresponds to the time component $x^0 = ct$ and $\mu = 1$ is associated with the space component $x^1 = x$. The DCS then reads [57]

$$\left(i\hbar\gamma^a e^\mu_{(a)}\partial_\mu + \frac{i\hbar}{2}\gamma^a\frac{1}{\sqrt{-g}}\partial_\mu(\sqrt{-g}e^\mu_{(a)}) - mc\right)\psi = 0, \quad (2)$$

where the matrices γ^a are given by the standard Pauli matrices $\gamma^0 = \sigma_z$ and $\gamma^1 = i\sigma_y$, and where $e^{(a)}_\mu$ is a dyad defined as $e^{(a)}_\mu = \partial X^a/\partial x^\mu$, with X^a (x^μ) denoting the a component (μ component) of the position vector in the Minkowski spacetime (curved spacetime). Dyads satisfy the orthonormality conditions $e^{(a)}_\mu e^\nu_{(a)} = \delta^\nu_\mu$. Now, we consider a semiclassical gravity theory in $(1+1)$ dimensions for a static point source. Notice that in $(1+1)$ dimensions all metrics are conformally flat, and Einstein's equations demand that it be an empty space. There are however interesting modifications of Einstein gravity. In particular, we consider the theory in which the curvature is proportional to the trace of the energy momentum tensor [46,58,59]. The metric is given by $g_{\mu\nu} = \mathrm{diag}[\alpha(x), -1/\alpha(x)]$ with $g_{00} = \alpha(x) = 2M|x| + \epsilon$, where M is related to the mass of the point source (in units of inverse length) $M = 4\pi G\rho_0 a/c^2$ with ρ_0 the density and a the spatial distribution radius of the dust, resulting in a total mass for the source of $\rho_0 a$, and where G is the $(1+1)$-dimensional gravitational constant, which in the Systeme International has units of $\mathrm{kg}^{-1}\,\mathrm{m}^1\,\mathrm{s}^{-2}$. For the constant value $\epsilon = +1$, the solution corresponds to the metric induced by a naked source. For $\epsilon = -1$, it corresponds to the exterior black hole solution. In this Letter, we show that the DCS in Eq. (2) for the black hole solution can be exactly mapped onto a multiphoton QRM in Eq. (1). Similarly, one can show that the naked source solution can also be mapped to the multiphoton QRM in the weak field approximation $2M|x| \ll 1$, see Ref. [60].

Mapping for the black hole solution.—Taking $\epsilon = -1$, we have $\alpha(x) = (|x| - r_s)/r_s$, where the corresponding Schwarzschild radius occurs at $r_s = 1/(2M)$, which is $r_s = c^2/(4\pi G\rho_0 a)$ in Systeme International units. Since the particle cannot cross the black hole at $x = 0$, it is restricted to a region either to the right or to the left of the origin. Here, we restrict the position of the particle to $x > r_s$, which can be done with no loss of generality due to the symmetry of the metric about the origin. This also means that the gravitational redshift factor $\sqrt{g_{00}} = \sqrt{\alpha}$ is restricted to positive values. In order to rewrite Eq. (2), we introduce operators $\hat{X}$ and $\hat{P}$ to carry out a mapping of the form

$$\hat{X} \equiv r_s\sqrt{\alpha(\hat{x})}, \qquad \hat{P} \equiv -i\hbar\frac{\partial}{\partial X}. \quad (3)$$

These operators are canonically conjugate and satisfy the commutation relation $[\hat{X}, \hat{P}] = i\hbar$. Under this mapping, the DCS in Eq. (2) becomes [60]

$$i\hbar\frac{\partial}{\partial t}\psi = \left(c\sigma_x\frac{1}{4r_s}\{\hat{X}, \hat{P}\} + mc^2\sigma_z\frac{\hat{X}}{r_s}\right)\psi, \quad (4)$$

where the operator $\{\hat{X}, \hat{P}\}$ acts as the generator of squeezing (see below). Alternatively, Eq. (4) can be derived choosing the polar coordinates (X, ct), in terms of which the spacetime interval reads $ds^2 = (X^2/r_s^2)c^2dt^2 - 4dX^2$, see Ref. [60]. The new $\hat{X}$ and $\hat{P}$ operators can be mapped to a bosonic field

$$\hat{X} = \frac{\lambda}{\sqrt{2}}(\hat{a} + \hat{a}^\dagger), \qquad \hat{P} = \frac{\hbar}{i\lambda\sqrt{2}}(\hat{a} - \hat{a}^\dagger), \quad (5)$$

where λ is a constant with units of length. Substituting expressions (5) in Eq. (4) we arrive at $i\hbar(\partial/\partial t)\psi = H_D\psi$ with the Hamiltonian

$$\hat{H}_D = \left(c\sigma_x\frac{1}{4ir_s}(\hat{a}^2 - \hat{a}^{\dagger 2}) + mc^2\sigma_z\frac{\lambda}{\sqrt{2}r_s}(\hat{a} + \hat{a}^\dagger)\right), \quad (6)$$

which is formally equivalent to the multiphoton QRM in Eq. (1) with $\omega = \omega_0 = 0$. Thus, Eq. (6) encodes the simulation of a Dirac particle in the background of a $(1+1)$-dimensional black hole. We point out that the inverse of the Schwarzschild radius $1/r_s$ appears as a multiplicative constant of Hamiltonian (6) and therefore multiplies the time variable in the corresponding unitary evolution operator. As a result, the simulation for a specific value of r_s is tantamount to the simulation for any value of

r_s up to a suitable rescaling of t. On the other hand, finding an analogy between the QRM and the DCS in higher dimensions seems a daunting task.

Trapped-ion implementation and numerical tests.—A trapped ion offers suitable quantum degrees of freedom for the simulation of Eq. (6), with its mechanical modes behaving as quantum harmonic oscillators that can hold the Hilbert space associated with operators a and $a^\dagger$, and two of its electronic states implementing the Hilbert space associated with Pauli operators.

To simplify the implementation, we change the σ_z Pauli operator in the second term of Eq. (6) into a σ_y, without altering the physics of the model. We propose to implement the term $[mc^2\lambda/(\sqrt{2}r_s)]\sigma_y(a+a^\dagger)\psi$ with red and blue sideband interactions, using Hamiltonians $-i\eta\Omega_r(\sigma^+a-\sigma^-a^\dagger)$ and $i\eta\Omega_b(\sigma^+a^\dagger-\sigma^-a)$, respectively. The corresponding Rabi frequencies are

$$\eta\Omega_r = mc^2\lambda/(\sqrt{2}r_s), \qquad \eta\Omega_b = -mc^2\lambda/(\sqrt{2}r_s). \tag{7}$$

Similarly, the term $[\hbar c/(4ir_s)]\sigma_x[a^2-(a^\dagger)^2]\psi$ can be implemented with red and blue second sidebands, $-i\eta_2^2\Omega_{r,2}[\sigma^+a^2-\sigma^-(a^\dagger)^2]$ and $i\eta_2^2\Omega_{b,2}[\sigma^+(a^\dagger)^2-\sigma^-a^2]$ with $\eta_2^2\Omega_{r,2}=\eta_2^2\Omega_{b,2}=\hbar c/(4r_s)$. Note that the values of Rabi frequencies $\Omega_{r(b)}$ and Lamb-Dicke parameters η for first and second sidebands can be set individually, given that these will be excited with independent laser fields, and therefore the ratio between first and second sideband interaction strengths can be set at will.

The position of the simulated Dirac particle at time t can be associated with observables of the mechanical degrees of freedom of the ion through the equivalence $(1/r_s)\hat{X}(t)^2 \equiv \hat{x}(t)-r_s$, where $\hat{x}(t)$ and $\hat{X}(t)^2$ are given in the Heisenberg representation. Similarly, the position of the ion moving in the trap can be associated with the redshift factor multiplied by r_s and with the position of the Dirac particle using the polar coordinates (t,X) as mentioned above. From an experimental point of view, the position of a trapped ion as well as higher order moments can be measured by mapping the information of the motional state of the ion to its internal degrees of freedom. Such measurements suffice to reconstruct the density profile of the ion as done in Refs. [42,56,63].

We consider the initial state $|\Psi_0\rangle = |\phi_0\rangle \otimes |\chi\rangle$, where $|\phi_0\rangle$ and $|\chi\rangle$ are, respectively, the wave functions of the spatial and internal degrees of freedom of the ion, which are unentangled at time $t=0$. We numerically simulate the unitary evolution of such a state under Hamiltonian (6) and track the expectation value $\langle X^2\rangle(t)$, related to the mechanical degrees of freedom of the ion. From it, we compute the expectation value of the position operator of the simulated Dirac particle, x. Note that for the semiclassical approximation to hold, the Compton wavelength of the Dirac particle $\lambda_c = h/(mc)$ must be much smaller than the Schwarzschild radius, $\lambda_c \ll r_s$. In Fig. 1 we show numerical results for the case of a massive particle; specifically, we analyze the regime in which $m=0.3/\lambda$ and $M=0.01/\lambda$, with $c=1$. The ion is initialized with its internal state in $|+\rangle_x$, where $|\pm\rangle_x$ are eigenstates of $\hat{\sigma}_x$. A Gaussian distribution $\phi_{X_0}(X) \equiv \langle X|\phi_0\rangle = \mathcal{N}e^{-[(X-X_0)^2/2\sigma^2]}$ describes the initial state of the mechanical degrees of freedom localized in half-space $X>0$, with values $X_0/\lambda=8$ and $\sigma/\lambda=1$ corresponding to a vacuum state displaced by $\alpha/\lambda=8$, and where $\mathcal{N}$ denotes the normalization factor. The trapped ion can be prepared in such an initial motional state by simultaneously applying resonant red and blue sidebands on it, when it is in its lower energy state [64], or via Bang-Bang techniques [65]. After changing the space variable $X(x) \equiv r_s\sqrt{\alpha(x)} = r_s\sqrt{(x/r_s)-1}$, we find that the corresponding initial wave function localized in the region $x>r_s$ for the simulated Dirac particle is given by $\phi_{x_0}(x) \equiv \langle x|\phi_0\rangle = [\partial X(x)/\partial x]^{1/2}\phi_{X_0}(X(x))$, where $x_0 \equiv (X_0^2/r_s)+r_s$.

Zitterbewegung effect in the presence of gravity.—As shown in Fig. 1(a), the simulated Dirac particle approaches asymptotically the horizon of the black hole at $x=r_s$. As the validity of our mapping is preserved throughout the entire time evolution, the ion does not cross the origin $X=0$, see Fig. 1(b). In addition, the ion trajectory exhibits

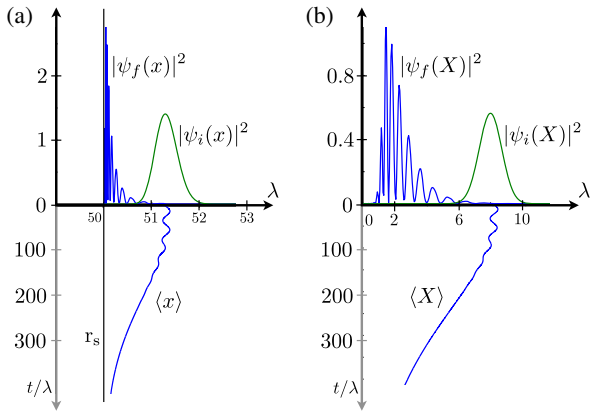

FIG. 1. Dynamics of a massive Dirac particle near a black hole and the multiphoton QRM. Properties of the simulated Dirac particle (a) are related to those of the ion (b), under the mapping (3). In both cases the upper plot shows the initial (green) and final (blue) probability density profiles, while the lower plots show the expectation values of the corresponding position operators. For the simulated Dirac particle, the position of the horizon is indicated by a vertical line labeled r_s. The initial state of the ion is $\Psi_0 = \phi_{X_0/\lambda=8}(X) \otimes |+\rangle_x$, where $\phi_{X_0/\lambda=8}(X)$ is a Gaussian wave function centered at X_0, and $|+\rangle_x$ is the eigenstate of operator σ_x with positive eigenvalue. The simulation is performed under the Hamiltonian in Eq. (6), for the case where $m\lambda=0.3$ and $M\lambda=0.01$, with $c=1$. The scale of the oscillations of the simulated particle is smaller than that of the oscillations of the ion, as the position of the simulated particle is rescaled by $1/r_s$ under mapping in Eq. (3).

an oscillatory behavior, with an amplitude that vanishes when the particle approaches the horizon. We associate this phenomenon with the *Zitterbewegung* effect, well known for massive relativistic fermions in flat spacetime, and originating from the interference between positive and negative energy solutions of the Dirac equation. We show that such a phenomenon persists in the presence of gravity. Intuitively, one can argue that this is indeed the case as a curved spacetime can be described locally by a Minkowski metric, in which we know that the particle manifests the *Zitterbewegung* effect. The equation of motion for the expectation value of the position operator $\hat{x}(t)$ reads [60]

$$\frac{d^2}{dt^2}\langle\hat{x}(t)\rangle = \frac{c^2}{r_s}\left(\frac{\langle\hat{x}(t)\rangle}{r_s} - 1\right) - \frac{2mc^3}{\hbar}\left\langle\left(\frac{\hat{x}(t)}{r_s} - 1\right)^{3/2} e^{2i\hat{H}_D t/\hbar}\hat{\sigma}_y\right\rangle, \quad (8)$$

where the second term, which depends on the mass, induces the oscillations in Fig. 1(a). In Ref. [60] we show that the amplitude of the oscillations decreases as the particle approaches the horizon $\langle\hat{x}(t)\rangle \to r_s$, see also Fig. 1(a). Our mapping offers an alternative way to observe the *Zitterbewegung* effect based on the recorded values of the redshift factor $\langle\hat{X}(t)\rangle/r_s$, see Fig. 1(b). Indeed, oscillations between red and blue shifts provide a direct signature of the *Zitterbewegung* effect. Note however that for a massless particle $m = 0$ this term vanishes, suppressing the *Zitterbewegung* effect, as expected [41,60]. In the massless case, an ion initialized with internal state $|+(-)\rangle_x$, i.e., in the positive (negative) chirality, moves away from the origin (towards the horizon).

Figure 1 further shows an interference pattern in the density profile that appears all along the dynamics. We identify this phenomenon as an additional signature of the *Zitterbewegung* effect. Indeed, this can be understood as an interference between positive and negative energy solutions of the Dirac equation that persists at long time. In flat spacetime positive and negative energy solutions spread in opposite directions and therefore do not overlap at long times. However, in the presence of gravity the two solutions approach the horizon (without crossing it). This results in the spatial squeezing of the density profile of the particle shown in Fig. 1. The overlap between both positive and negative energy solutions is therefore maximized as the particle approaches the horizon and the oscillations in the trajectory are suppressed. We note that for the massless case the interference pattern in the density profile is absent (see Ref. [60]), consistently with the suppression of the *Zitterbewegung* effect.

Squeezed states and gravity.—To understand the spatial squeezing of the density profile (see Fig. 1), we stress that the mapping we introduce, see Eqs. (4)–(6), suggests an analogy between squeezing in quantum optics and curvature of spacetime in the context of the relativistic Dirac equation. From this analogy, we expect that gravity generates squeezed states as time evolves. A standard way to characterize squeezing along the dynamics is to look at the time evolution of the variance of the position and the momentum, $\Delta X(t)$ and $\Delta P(t)$ [defined for an arbitrary operator O as $\Delta O(t) \equiv \sqrt{\langle\hat{O}(t)^2\rangle - \langle\hat{O}(t)\rangle^2}$]. In Fig. 2 we show that the variance of the momentum of the ion $\Delta\hat{P}(t)$ grows indefinitely when the particle approaches the horizon of the black hole while the variance of the position $\Delta\hat{X}(t)$ decreases and tends asymptotically to zero. This gives a signature of the squeezing of the wave function when the particle approaches the horizon. A similar squeezing is observed as well in the massless case, as we show in Ref. [60]. Note that the relation between squeezing and gravity has been recently explored in the context of cosmological particle creation [47], in analogues using Bose-Einstein condensates [11,48,66] and trapped ions [49], and in relation to the Hawking effect near a Schwarzschild black hole [47,50]. However, our results exploit the first-quantization formalism, and therefore the predicted squeezing relates exclusively to the phase space of the simulated particle and cannot be, *a priori*, associated with cosmological particle creation.

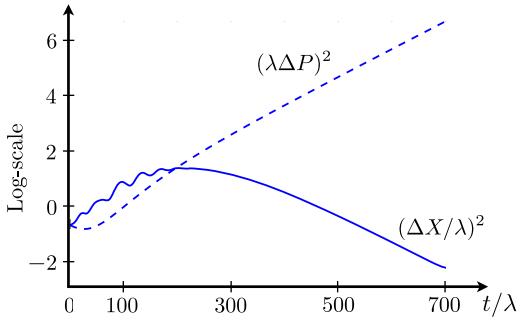

FIG. 2. Squeezing of the dynamics by curvature of spacetime. The continuous line corresponds to the variance of the position of the ion $(\Delta X/\lambda)^2$ while the dashed line corresponds to the variance of the momentum of the ion $(\lambda\Delta P)^2$, both being dimensionless. A logarithmic scale is used. The simulation regime is the same as that in Fig. 1. As the ion evolves in time a clear trend towards its position getting localized accompanied with an exponential growth of the uncertainty of its momentum can be observed.

Conclusions.—We have proposed an analogy between the DCS and a multiphoton QRM. We have shown that the former can be exactly mapped to the latter when the metric describes a $(1+1)$-dimensional analogue of a Schwarzschild black hole. We have proposed the implementation of the mapping with a single trapped ion and used numerical results to illustrate the dynamics of the ion and a simulated Dirac particle. Our results show that the *Zitterbewegung* effect in curved spacetime leads to the oscillatory trajectory of the ion and the interference pattern in its probability density profile. In addition, our findings demonstrate that gravitation and quantum squeezing are

strongly related and we hope that our present work will motivate further research in this direction. The analogy presented here illustrates a connection between relativistic quantum mechanics in curved spacetimes and basic light-matter interaction models, which may inspire quantum simulations of relativistic equations in curved spacetimes in a variety of quantum platforms.

We acknowledge support from Spanish Ministerio de Economía y Competitividad/Fondo Europeo de Desarrollo Regional FIS2015-69983-P, Basque Government IT986-16, Ramón y Cajal Grant No. RYC-2012-11391, UMass Boston (Project No. P20150000029279), and the John Templeton Foundation.

[1] W. G. Unruh, Phys. Rev. Lett. **46**, 1351 (1981).
[2] M. Visser, arXiv:gr-qc/9311028.
[3] W. G. Unruh, Phys. Rev. D **51**, 2827 (1995).
[4] M. Visser, Classical Quantum Gravity **15**, 1767 (1998).
[5] R. Schützhold and W. G. Unruh, Phys. Rev. D **66**, 044019 (2002).
[6] G. Rousseaux, C. Mathis, P. Maïssa, T. G. Philbin, and U. Leonhardt, New J. Phys. **10**, 053015 (2008).
[7] S. Weinfurtner, E. W. Tedford, M. C. J. Penrice, W. G. Unruh, and G. A. Lawrence, Phys. Rev. Lett. **106**, 021302 (2011).
[8] L. J. Garay, J. R. Anglin, J. I. Cirac, and P. Zoller, Phys. Rev. Lett. **85**, 4643 (2000).
[9] C. Barceló, S. Liberati, and M. Visser, Classical Quantum Gravity **18**, 1137 (2001).
[10] L. Garay, Int. J. Theor. Phys. **41**, 2073 (2002).
[11] C. Barceló, S. Liberati, and M. Visser, Phys. Rev. A **68**, 053613 (2003).
[12] P. O. Fedichev and U. R. Fischer, Phys. Rev. Lett. **91**, 240407 (2003).
[13] P. O. Fedichev and U. R. Fischer, Phys. Rev. D **69**, 064021 (2004).
[14] U. R. Fischer, Mod. Phys. Lett. A **19**, 1789 (2004).
[15] U. R. Fischer and R. Schützhold, Phys. Rev. A **70**, 063615 (2004).
[16] S. Giovanazzi, C. Farrell, T. Kiss, and U. Leonhardt, Phys. Rev. A **70**, 063602 (2004).
[17] O. Lahav, A. Itah, A. Blumkin, C. Gordon, S. Rinott, A. Zayats, and J. Steinhauer, Phys. Rev. Lett. **105**, 240401 (2010).
[18] J. Steinhauer, Nat. Phys. **12**, 959 (2016).
[19] S.-Y. Chä and U. R. Fischer, Phys. Rev. Lett. **118**, 130404 (2017).
[20] J. Rodríguez-Laguna, L. Tarruell, M. Lewenstein, and A. Celi, Phys. Rev. A **95**, 013627 (2017).
[21] G. Volovik, Czech J. Phys. **46**, 3048 (1996).
[22] G. Volovik, J. Low Temp. Phys. **113**, 667 (1998).
[23] T. A. Jacobson and G. E. Volovik, Phys. Rev. D **58**, 064021 (1998).
[24] F. Baldovin, M. Novello, S. P. Bergliaffa, and J. Salim, Classical Quantum Gravity **17**, 3265 (2000).
[25] M. Novello, V. A. De Lorenci, J. M. Salim, and R. Klippert, Phys. Rev. D **61**, 045001 (2000).
[26] V. De Lorenci, R. Klippert, M. Novello, and J. Salim, Phys. Lett. B **482**, 134 (2000).
[27] V. A. De Lorenci, R. Klippert, M. Novello, and J. M. Salim, Phys. Rev. D **65**, 063501 (2002).
[28] A. V. Arellano and F. S. Lobo, Classical Quantum Gravity **23**, 5811 (2006).
[29] U. Leonhardt and P. Piwnicki, Phys. Rev. Lett. **84**, 822 (2000).
[30] I. Brevik and G. Halnes, Phys. Rev. D **65**, 024005 (2001).
[31] U. Leonhardt, Nature (London) **415**, 406 (2002).
[32] W. G. Unruh and R. Schützhold, Phys. Rev. D **68**, 024008 (2003).
[33] R. Schützhold and W. G. Unruh, Phys. Rev. Lett. **95**, 031301 (2005).
[34] C. Koke, C. Noh, and D. G. Angelakis, Ann. Phys. (Berlin) **374**, 162 (2016).
[35] B. Horstmann, B. Reznik, S. Fagnocchi, and J. I. Cirac, Phys. Rev. Lett. **104**, 250403 (2010).
[36] F. Belgiorno, S. l. Cacciatori, M. Clerici, V. Gorini, G. Ortenzi, L. Rizzi, E. Rubino, V. G. Sala, and D. Faccio, Phys. Rev. Lett. **105**, 203901 (2010).
[37] W. G. Unruh and R. Schützhold, Phys. Rev. D **86**, 064006 (2012).
[38] C. Barceló, S. Liberati, and M. Visser, Living Rev. Relativity **14**, 3 (2011).
[39] D. Faccio, F. Belgiorno, S. Cacciatori, V. Gorini, S. Liberati, and U. Moschella, *Analogue Gravity Phenomenology: Analogue Spacetimes and Horizons, from Theory to Experiment*, Vol. 870 (Springer, New York, 2013).
[40] C. Sabín, arXiv:1707.05519.
[41] L. Lamata, J. León, T. Schätz, and E. Solano, Phys. Rev. Lett. **98**, 253005 (2007).
[42] R. Gerritsma, G. Kirchmair, F. Zahringer, E. Solano, R. Blatt, and C. F. Roos, Nature (London) **463**, 68 (2010).
[43] J. S. Pedernales, I. Lizuain, S. Felicetti, G. Romero, L. Lamata, and E. Solano, Sci. Rep. **5**, 15472 (2015).
[44] T. Salger, C. Grossert, S. Kling, and M. Weitz, Phys. Rev. Lett. **107**, 240401 (2011).
[45] J. C. Garreau and V. Zehnlé, Phys. Rev. A **96**, 043627 (2017).
[46] R. B. Mann, S. M. Morsink, A. E. Sikkema, and T. G. Steele, Phys. Rev. D **43**, 3948 (1991).
[47] T. Jacobson, in *Lectures on Quantum Gravity*, edited by A. Gomberoff and D. Marolf (Springer US, Boston, MA, 2005), pp. 39–89.
[48] E. A. Calzetta and B. L. Hu, Phys. Rev. A **68**, 043625 (2003).
[49] R. Schützhold, M. Uhlmann, L. Petersen, H. Schmitz, A. Friedenauer, and T. Schätz, Phys. Rev. Lett. **99**, 201301 (2007).
[50] D. Su, C. T. Marco Ho, R. B. Mann, and T. C. Ralph, Phys. Rev. D **96**, 065017 (2017).
[51] D. Lv, S. An, Z. Liu, J.-N. Zhang, J. S. Pedernales, L. Lamata, E. Solano, and K. Kim, arXiv:1711.00582.
[52] A. Mezzacapo, U. Las Heras, J. S. Pedernales, L. DiCarlo, E. Solano, and L. Lamata, Sci. Rep. **4**, 7482 (2015).
[53] J. Braumüller, M. Marthaler, A. Schneider, A. Stehli, H. Rotzinger, M. Weides, and A. V. Ustinov, Nat. Commun. **8**, 779 (2017).
[54] N. K. Langford, R. Sagastizabal, M. Kounalakis, C. Dickel, A. Bruno, F. Luthi, D. J. Thoen, A. Endo, and L. DiCarlo, Nat. Commun. **8**, 1715 (2017).

[55] S. Felicetti, J. S. Pedernales, I. L. Egusquiza, G. Romero, L. Lamata, D. Braak, and E. Solano, Phys. Rev. A **92**, 033817 (2015).
[56] R. Gerritsma, B. P. Lanyon, G. Kirchmair, F. Zähringer, C. Hempel, J. Casanova, J. J. García-Ripoll, E. Solano, R. Blatt, and C. F. Roos, Phys. Rev. Lett. **106**, 060503 (2011).
[57] G. C. McVittie, Mon. Not. R. Astron. Soc. **92**, 868 (1932).
[58] R. B. Mann, Found. Phys. Lett. **4**, 425 (1991).
[59] R. B. Mann, Gen. Relativ. Gravit. **24**, 433 (1992).
[60] See Supplemental Material at http://link.aps.org/supplemental/10.1103/PhysRevLett.120.160403 for additional information, which includes Refs. [61,62].
[61] A. Bermudez, M. A. Martin-Delgado, and E. Solano, Phys. Rev. A **76**, 041801 (2007).
[62] M. Arminjon and F. Reifler, Braz. J. Phys. **43**, 64 (2013).
[63] F. Zähringer, G. Kirchmair, R. Gerritsma, E. Solano, R. Blatt, and C. F. Roos, Phys. Rev. Lett. **104**, 100503 (2010).
[64] D. M. Meekhof, C. Monroe, B. E. King, W. M. Itano, and D. J. Wineland, Phys. Rev. Lett. **76**, 1796 (1996).
[65] J. Alonso, F. M. Leupold, Z. U. Solèr, M. Fadel, M. Marinelli, B. C. Keitch, V. Negnevitsky, and J. P. Home, Nat. Commun. **7**, 11243 (2016).
[66] P. O. Fedichev and U. R. Fischer, Phys. Rev. A **69**, 033602 (2004).